In vivo visualization of tau deposits in corticobasal syndrome by ^{18}F-THK5351 PET

Akio Kikuchi, MD, PhD*
Nobuyuki Okamura, MD, PhD*
Takafumi Hasegawa, MD, PhD
Ryuichi Harada, PhD
Shoichi Watanuki
Yoshihito Funaki, PhD
Kotaro Hiraoka, MD, PhD
Toru Baba, MD, PhD
Naoto Sugeno, MD, PhD
Ryuji Oshima, MD, PhD
Shun Yoshida, MD
Junpei Kobayashi, MD
Michinori Ezura, MD
Michiko Kobayashi, MD, PhD
Ohito Tano, MD
Shunji Mugikura, MD, PhD
Ren Iwata, PhD
Aiko Ishiki, MD, PhD
Katsutoshi Furukawa, MD, PhD
Hiroyuki Arai, MD, PhD
Shozo Furumoto, PhD
Manabu Tashiro, MD, PhD
Kazuhiko Yanai, MD, PhD
Yukitsuka Kudo, PhD
Atsushi Takeda, MD, PhD
Masashi Aoki, MD, PhD

Correspondence to Dr. Kikuchi: akikuchi@med.tohoku.ac.jp or Dr. Okamura: nookamura@med.tohoku.ac.jp

Supplemental data at Neurology.org

ABSTRACT

Objective: To determine whether ^{18}F-THK5351 PET can be used to visualize tau deposits in brain lesions in live patients with corticobasal syndrome (CBS).

Methods: We evaluated the in vitro binding of ^{3}H-THK5351 in postmortem brain tissues from a patient with corticobasal degeneration (CBD). In clinical PET studies, ^{18}F-THK5351 retention in 5 patients with CBS was compared to that in 8 age-matched normal controls and 8 patients with Alzheimer disease (AD).

Results: ^{3}H-THK5351 was able to bind to tau deposits in the postmortem brain with CBD. In clinical PET studies, the 5 patients with CBS showed significantly higher ^{18}F-THK5351 retention in the frontal, parietal, and globus pallidus than the 8 age-matched normal controls and patients with AD. Higher ^{18}F-THK5351 retention was observed contralaterally to the side associated with greater cortical dysfunction and parkinsonism.

Conclusions: ^{18}F-THK5351 PET demonstrated high tracer signal in sites susceptible to tau deposition in patients with CBS. ^{18}F-THK5351 should be considered as a promising candidate radiotracer for the in vivo imaging of tau deposits in CBS. ***Neurology*® 2016;87:2309–2316**

GLOSSARY

AD = Alzheimer disease; **CBD** = corticobasal degeneration; **CBS** = corticobasal syndrome; **DAT** = dopamine transporter; **H/M** = heart to mediastinum; **MIBG** = ^{123}I-metaiodobenzylguanidine; **MMSE** = Mini-Mental State Examination; **PiB** = Pittsburgh compound B; **PSP** = progressive supranuclear palsy; **SBR** = specific binding ratio; **SUV** = standardized uptake value; **SUVR** = standardized uptake value ratio; **THK5352** = (*S*)-2-(2-methylaminopyrid-5-yl)-6-[[2-(tetrahydro-2H-pyran-2-yloxy)-3-tosyloxy]propoxy] quinoline; **VOI** = volume of interest.

Corticobasal syndrome (CBS) is an asymmetric higher cortical dysfunction manifested as parkinsonism, dystonia, and myoclonus.[1–3] The underlying neuropathology for the CBS phenotype includes corticobasal degeneration (CBD), progressive supranuclear palsy (PSP), Alzheimer disease (AD), frontotemporal lobar degeneration, Parkinson disease, and Creutzfeldt-Jakob disease. The frequency of underlying pathology in CBS varies and approximately half of the CBS cases present with CBD (CBS-CBD). Cortical variant PSP (CBS-PSP) and AD (CBS-AD) are each associated with about 20% of CBS cases.[3,4] The intracellular fibrillary tangles observed in CBD and PSP are composed of 4-repeat tau, whereas both 3- and 4-repeat tau isoforms accumulate in AD.

The radiotracers used to image tau neurofibrillary tangle deposition in the living typical AD brain are ^{18}F-FDDNP,[5] ^{18}F-AV1451 (T807),[6] ^{11}C-PBB3,[7] and a series of ^{18}F-THK compounds, such as ^{18}F-THK523,[8] ^{18}F-THK5105,[9] ^{18}F-THK5117,[10] and ^{18}F-THK5351.[11] We do not yet know whether these radiotracers detect tau deposits in vivo in patients with CBS. ^{18}F-FDDNP accumulated in the subthalamic area, midbrain region, and cerebellar white matter of a patient with classical PSP, but not in patients with CBS-PSP.[12] An ^{11}C-PBB3 PET imaging study also

*These authors contributed equally to this work.

From the Departments of Neurology (A.K., T.H., T.B., N.S., R.O., S.Y., J.K., M.E., M.A.), Pharmacology (N.O., R.H., K.Y.), and Diagnostic Radiology (S.M.), Tohoku University Graduate School of Medicine; Divisions of Cyclotron Nuclear Medicine (S.W., K.H., M.T.) and Radiopharmaceutical Chemistry (Y.F., R.I., S.F.), Cyclotron and Radioisotope Center, and Department of Geriatric and Respiratory Medicine (A.I., K.F., H.A.) and Division of Neuroimaging (Y.K.), Institute of Development, Aging and Cancer, Tohoku University; Department of Neurology (M.K.), Tohoku Pharmaceutical University Hospital; Department of Neurology (O.T.), Sendai Medical Center; and Department of Neurology (A.T.), National Hospital Organization, Sendai Nishitaga Hospital, Sendai, Japan.

Go to Neurology.org for full disclosures. Funding information and disclosures deemed relevant by the authors, if any, are provided at the end of the article.

Figure 1 Autoradiography of ^{3}H-THK5351 and tau immunostaining in postmortem middle frontal gyrus sections from a 65-year-old woman with corticobasal degeneration

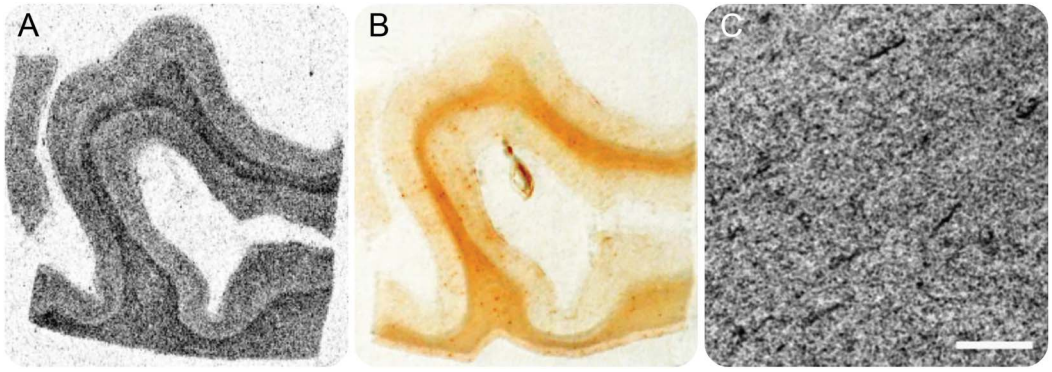

(A) The ^{3}H-THK5351 tracer and (B) tau (AT8) antibody staining colocalized with tau deposition in the subcortical white matter. (C) In the microautoradiography of the same brain section, ^{3}H-THK5351 bound to thread-like structures in the white matter. Scale bars are 100 μm.

indicated that tau accumulated in the neocortex and in subcortical structures, such as the basal ganglia, thalamus, and midbrain, in a patient with CBS,[7] although this observation has not been confirmed in a case-control study. ^{18}F-THK5351 is a novel radiotracer with a high binding affinity and selectivity for tau protein deposits.[11] We evaluated whether ^{18}F-THK5351 PET can selectively bind to tau pathology in living patients with CBS.

METHODS **Autoradiography.** THK5351 was synthesized from its tosylate precursor, (*S*)-2-(2-methylaminopyrid-5-yl)-6-[[2-(tetrahydro-2H-pyran-2-yloxy)-3-tosyloxy]propoxy] quinoline (THK5352), as described previously.[11,13] ^{3}H-THK5351 (specific activity, 2.96 TBq/mmol; radiochemical purity, 98.9%) was custom-labeled by Sekisui Medical Inc. (Tokyo, Japan).[11] Autoradiography in middle frontal gyrus postmortem brain sections from a 65-year-old woman with CBD was conducted using ^{3}H-THK5351 and tau (AT8) immunostaining, as described previously.[11] We estimated the concentration relationship between the ^{3}H-THK5351 autoradiography and tau (AT8) immunostaining in 5 regions of interest each of gray matter and white matter using the ImageQuant TL software (GE Healthcare, Piscataway, NJ).

Participants. Five patients with CBS (one male and 4 female, age 69.2 ± 7.0 years, age range 64–81 years, Mini-Mental State Examination [MMSE] score 20.0 ± 7.9), 8 age-matched normal controls (4 male and 4 female, age 71.1 ± 6.9 years, age range 61–81 years, MMSE score 28.6 ± 1.6), and 8 age-matched patients with amnestic AD (5 male and 3 female, age 76.6 ± 8.4 years, age range 64–88 years, MMSE score 18.1 ± 4.7) underwent ^{18}F-THK5351 PET scans. Probable CBS was diagnosed based on the modified Cambridge criteria.[14] All patients were right-handed. Three of the 5 patients had right-side dominant symptoms and 2 of them were left-side dominant. The Montreal Cognitive Assessment, Addenbrooke's Cognitive Examination–Revised, and Frontal Assessment Battery were used to assess the cognitive performance of the participants. Motor functions were assessed using the Unified Parkinson's Disease Rating Scale motor score and the PSP Rating Scale. We also examined the results of the Odor Stick Identification Test for Japanese, a CSF study, and ^{123}I-metaiodobenzylguanidine (MIBG) and dopamine transporter (DAT) scans. The normal control group comprised volunteers with no cognitive or motor function impairments, who did not have any observable cerebrovascular lesions as indicated by MRI scans. Probable AD was diagnosed based on the criteria of the National Institute of Neurologic and Communicative Disorders and Stroke and the Alzheimer's Disease Related Disorders Association. Some of the data from normal controls and patients with AD were presented in our previous article.[11]

Standard protocol approvals, registrations, and patient consents. The study protocol was approved by the Ethics Committee of the Tohoku University Hospital (approval number: 2014-2-159) and was registered to the UMIN Clinical Trial Registry (registration number: UMIN000013929). Written informed consent was obtained from each patient or his or her guardians after they were given a complete description of the study.

Image acquisition. ^{18}F-THK5351 and ^{11}C-Pittsburgh compound B (PiB) was prepared at the Cyclotron and Radioisotope Center of Tohoku University using a semiautomated system developed in-house. Injectable solutions of ^{18}F-THK5351 and ^{11}C-PiB were obtained at a radiochemical purity of >95% and a specific activity of 357 ± 270 and 240 ± 48 GBq/μmol. PET imaging was performed using an Eminence STARGATE scanner (Shimadzu, Kyoto, Japan). After injecting 185 MBq of ^{18}F-THK5351 or 296 MBq of ^{11}C-PiB, PET images were obtained for 20 minutes (4 scans × 300 seconds) from 40 to 60 minutes or from 50 to 70 minutes postinjection and were used for further analysis. A 3D volumetric acquisition of a T1-weighted gradient echo sequence produced a gapless series of thin axial sections using a spoiled gradient recall sequence (echo time/repetition time, 3.4/7.2 ms; flip angle, 9°; acquisition matrix, 240 × 256; 1 excitation; field of view, 25.6 cm; slice thickness, 0.8 mm) of a Vantage Titan TM 3T scanner (Toshiba Medical Systems, Otawara, Japan).

Cardiac planar images of ^{123}I-MIBG myocardial scintigraphy were acquired 25 minutes (early image) and 3 hours (delayed image) after an IV injection of 111 MBq of ^{123}I-MIBG (FUJIFILM RI Pharma Co., Ltd., Tokyo, Japan) using a Symbia-T (Siemens,

Table 1 Demographic characteristics of patients with corticobasal syndrome (CBS)

	Case 1	Case 2	Case 3	Case 4	Case 5
Age, y/sex	70/F	81/F	64/M	67/F	64/F
Symptom duration	4 y, 6 mo	3 y, 0 mo	1 y, 5 mo	2 y, 7 mo	1 y, 7 mo
Symptom-dominant side	Right	Right	Right	Left	Left
Symptom					
Upward gaze limitation	++	+++	—	—	—
Retropulsion	+++	+++	—	—	—
Limb-kinetic apraxia (right/left)	+++/+	+++/++	++/—	—/++	++/+++
Ideomotor apraxia (right/left)	+++/++	+++/++	++/—	—/++	++/+++
Ideational apraxia (right/left)	+++/—	+++/++	—/—	—/+	++/+++
Constructional apraxia (right/left)	+++/++	+++/++	+/—	—/+	++/+++
Left hemispatial neglect	—	—	—	—	+
Alien hand	+	+	+	+	+
Transcortical motor aphasia	++	+	+	+	—
Motor aphasia	—	—	—	—	++
Transcortical sensory aphasia	—	—	—	—	—
Sensory aphasia	—	—	—	—	—
Cognitive scores					
MMSE score	13	15	27	30	15
MoCA score	7	4	19	29	8
ACE-R score	26	31	82	94	33
FAB score	3	1	14	15	5
Motor scores					
UPDRS (motor score)	103	77	47	22	75
PSPRS score	68	47	17	16	40
OSIT-J score	7	5	7	11	5
Imaging					
SBR in DAT scan (right/left)	4.2/1.9	4.4/3.6	2.5/1.3	5.7/6.4	1.8/3.2
H/M ratio in ^{131}I-MIBG (early/delay)	2.5/2.9	2.9/3.2	3.2/3.8	2.3/2.5	2.7/3.1
^{11}C-PiB SUVR in neocortex	1.22	2.17	1.10	1.46	1.16
CSF study					
p-tau (181) and total tau, pg/mL	41.1, 324	56.0, 486	32.6, 184	60.7, 464	36.2, 237
β-Amyloid 1–40 and 1–42, pg/mL	6,035, 963	10,757, 910	9,906, 1,256	9,035, 1,146	8,782, 954
β-Amyloid 1–42/(152 + 8.25 × p-tau)	1.96	1.48	2.98	1.76	2.12
p-tau/total tau	0.13	0.12	0.18	0.13	0.15

Abbreviations: + = Mild; ++ = moderate; +++ = severe; ACE-R = Addenbrooke's Cognitive Examination–Revised; DAT = dopamine transporter; FAB = Frontal Assessment Battery; H/M = heart-to-mediastinum; MIBG = meta-iodobenzylguanidine; MMSE = Mini-Mental State Examination; MoCA = Montreal Cognitive Assessment; OSIT-J score = Odor Stick Identification Test for the Japanese; PiB = Pittsburgh compound B; PSPRS = Progressive Supranuclear Palsy Rating Scale; SBR = specific binding ratio; SUVR = standardized uptake value ratio; UPDRS = Unified Parkinson's Disease Rating Scale.

Erlangen, Germany). DAT images were acquired 3 hours after an IV injection of 167 MBq of ^{123}I-ioflupane (Nihon Medi-Physics Co, Ltd., Tokyo, Japan) using a Symbia-E (Siemens).

Image analysis. Standardized uptake value (SUV) images of ^{18}F-THK5351 and ^{11}C-PiB were obtained by normalizing the tissue radioactivity concentration to the injected dose and body weight. The PNEURO module in PMOD software (version 3.6; PMOD Technologies, Zurich, Switzerland) was used to place and evaluate the volumes of interest (VOIs) using an automatic VOI method. The PET images were matched rigidly to the T1-weighted MRIs acquired from each participant. The MRIs were spatially normalized to the Montreal Neurological Institute T1 MRI template. VOIs were automatically outlined on the normalized MRI based on the maximum probability atlas constructed by Hammers et al., which is used in the

Figure 2 **^{18}F-THK5351 PET images overlaid on MRI data in a normal control participant and in 5 patients with corticobasal syndrome (CBS), surface projection maps showing areas with *Z* scores of more than 2.0, and regional ^{18}F-THK5351 standardized uptake value ratio (SUVR) values in a normal control and participants with CBS**

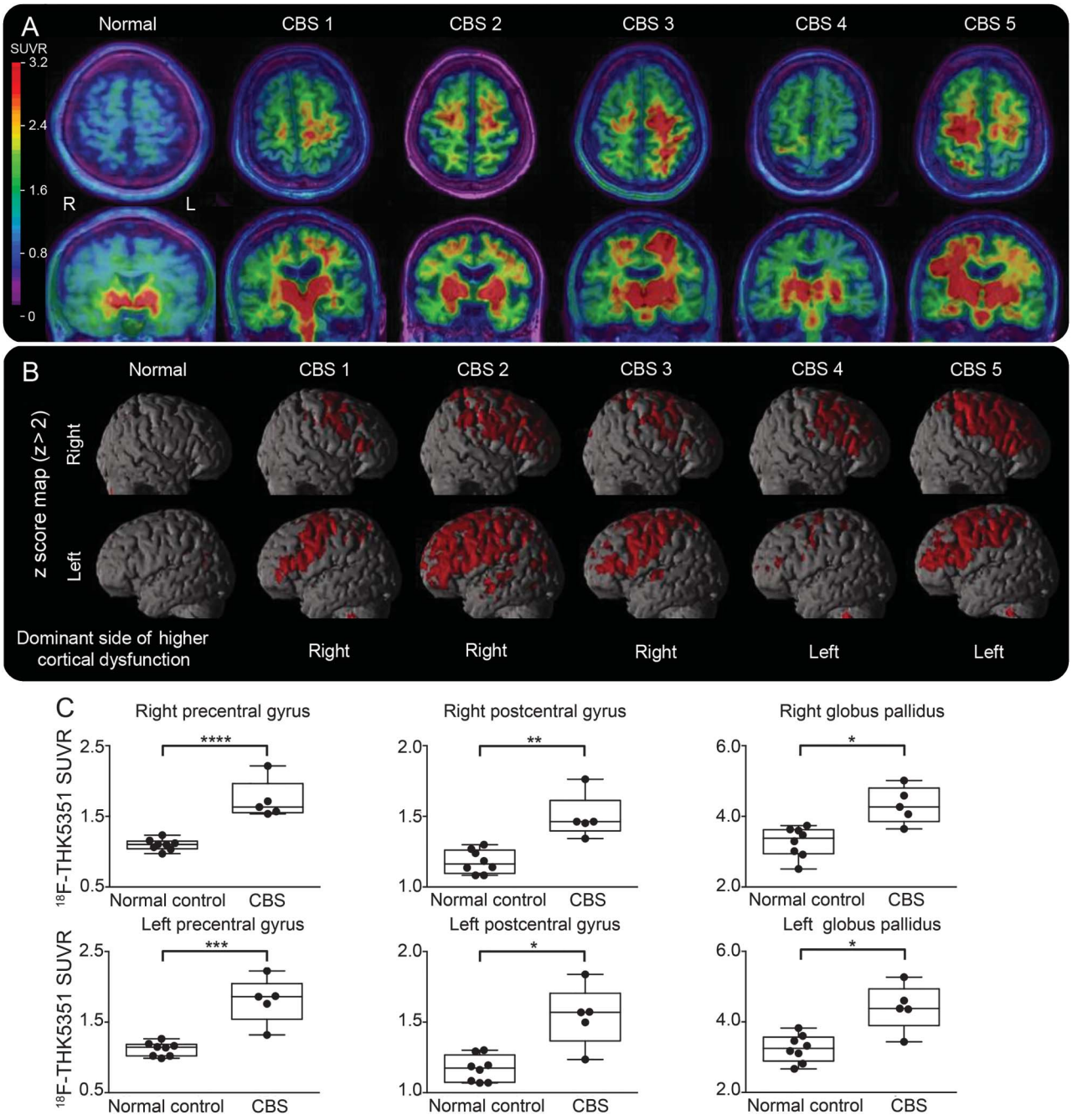

^{18}F-THK5351 retention in the precentral and postcentral gyri, globus pallidus, and putamen was more evident in patients with CBS than in the normal control. (A, B) In patients with CBS, a higher accumulation of ^{18}F-THK5351 was seen in regions contralateral to the symptom-predominant side. (C) There were significant differences in ^{18}F-THK5351 SUVR values of normal controls and patients with CBS in the bilateral precentral and postcentral gyri and globus pallidus. *$p < 0.005$, **$p < 0.001$, ***$p < 0.0005$, ****$p < 0.0001$ by Holm-Sidak multiple comparisons test.

PMOD software. VOIs were defined in the following regions: bilateral precentral, postcentral, superior frontal, superior parietal, and posterior cingulate gyri, globus pallidus, putamen, caudate nucleus, substantia nigra, middle and inferior temporal gyrus, hippocampus, amygdala, and cerebellar gray matter. The cerebellar gray matter was used as a reference region. The regional SUV to cerebellar cortex SUV ratio (SUVR) was used as an index of tracer retention. Neocortical β-amyloid burden was expressed as the average SUVR for the following cortical volumes of interest: superior frontal, superior parietal, middle and inferior temporal, and posterior cingulate gyri for ^{11}C-PiB. As in previous studies, an ^{11}C-PiB SUVR threshold of 1.5 was used to categorize high and low β-amyloid burden.[9,15,16] *Z* score maps were created using the mean and SD images from 8 normal controls. Voxel-based group comparisons between normal controls and patients with CBS or with AD and between patients with CBS and with AD were performed using statistical parametric mapping software

Table 2 Regional ^{18}F-THK5351 standardized uptake value ratio values in 5 patients with corticobasal syndrome

Region	Case 1	Case 2	Case 3	Case 4	Case 5
R precentral gyrus	1.54	1.71	1.63	1.57	2.21
L precentral gyrus	1.86	1.87	2.23	1.32	1.76
R postcentral gyrus	1.46	1.45	1.46	1.34	1.76
L postcentral gyrus	1.50	1.57	1.84	1.24	1.57
R globus pallidus	4.27	4.06	4.59	3.65	5.01
L globus pallidus	4.61	4.38	5.27	3.43	4.36
R putamen	3.05	3.61	3.54	3.05	3.84
L putamen	3.20	3.59	3.94	2.88	3.39
R caudate nucleus	1.93	2.08	2.36	2.19	2.54
L caudate nucleus	1.49	2.26	2.15	2.16	2.34
R substantia nigra	2.82	2.13	3.26	2.47	3.35
L substantia nigra	3.20	2.49	3.57	2.31	3.42
R middle inferior temporal gyrus	1.58	1.62	1.58	1.48	1.76
L middle inferior temporal gyrus	1.66	1.64	1.62	1.44	1.74
R hippocampus	2.34	2.25	2.45	2.32	2.46
L hippocampus	2.10	2.31	2.47	2.22	2.46
R amygdala	2.49	2.30	2.88	2.33	3.22
L amygdala	2.35	2.35	2.78	2.21	2.92
R superior frontal gyrus	1.53	1.74	1.61	1.57	1.85
L superior frontal gyrus	1.71	1.86	1.73	1.43	1.74
R superior parietal gyrus	1.59	1.72	1.53	1.42	2.04
L superior parietal gyrus	1.75	1.75	1.77	1.39	1.73
R posterior cingulate gyrus	1.81	1.76	1.69	1.64	1.94
L posterior cingulate gyrus	1.83	1.81	1.69	1.65	1.88

(SPM12; Wellcome Department of Imaging Neuroscience, UCL, London, UK).

Cardiac ^{123}I-MIBG accumulation was evaluated using the heart to mediastinum (H/M) ratio. Striatal ^{123}I-Ioflupane accumulation was evaluated by specific binding ratio (SBR) calculation using an occipital lobe as a background region.

Statistical analysis. We used a repeated-measures analysis of variance followed by Holm-Sidak multiple comparisons test to compare regional SUVR values of ^{18}F-THK5351 and ^{11}C-PiB in normal controls vs patients with CBS. Effect size coefficients (Cohen *d*) were calculated to evaluate group differences in the PET measurements. The analyses were performed using GraphPad Prism6 software (GraphPad, San Diego, CA). Data were expressed as mean ± SD.

RESULTS

Autoradiography in CBD. Autoradiography in a postmortem CBD patient brain showed a high density of ^{3}H-THK5351 binding in the subcortical white matter of the middle frontal gyrus (figure 1A), which corresponded to tau immunohistochemistry (figure 1B). Microautoradiography of the same section also showed ^{3}H-THK5351 binding to thread-like structures in the white matter (figure 1C). The concentration between the ^{3}H-THK5351 autoradiography and tau (AT8) staining showed linear relationship ($p < 0.005$, figure e-1 at Neurology.org).

Clinical features of patients with CBS. Table 1 summarizes the clinical features of the patients with CBS. Age was not significantly different among the 3 groups. As expected, we observed significant differences between the CBS and normal control groups in their MMSE scores. CBS cases showed no remarkable decrease in the levels of Aβ1–42 in CSF. In one study,[17] scores below 1 using the formula Aβ1–42/(152 + 8.25 × p-tau) in CSF showed AD at a high rate in 16 out of 17 cases, the diagnoses of which were confirmed by autopsy. All CBS cases showed a high score of more than 1 (table 1). DAT scans in 4 CBS patients, but not case 4, showed a "dot" appearance in the basal ganglia predominantly contralateral to the affected symptoms (data not shown) and SBR were less than 4.5 in 4 CBS patients except for case 4, which is not typically observed in AD. Both early and delayed H/M ratios of all CBS patients were greater than 2.2.

Clinical PET studies in healthy elderly controls and patients with CBS. ^{18}F-THK5351 PET images and *Z* score maps in a normal control (61-year-old female, MMSE score 30) and 5 patients with CBS are shown in figure 2, A and B. We observed ^{18}F-THK5351 retention in the precentral and postcentral gyri, and basal ganglia in patients with CBS (figure 2A). In all patients with CBS, a higher uptake of ^{18}F-THK5351 was seen in the contralateral precentral, postcentral, superior frontal, and superior parietal gyri of the symptom-predominant side (figure 2, A and B, and table 2). ^{18}F-THK5351 SUVR values for the bilateral precentral, postcentral, superior frontal, and superior parietal gyri and globus pallidus and left posterior cingulate gyrus were significantly greater in patients with CBS than in normal controls (figure 2C and tables 3 and e-1). On the other hand, no significant differences between the 2 groups were found in the bilateral caudate nuclei, substantia nigra, middle inferior temporal gyri, hippocampus, and amygdala or right posterior cingulate gyrus (table 3). We performed voxel-by-voxel comparisons of ^{18}F-THK5351 PET images in CBS, AD, and normal groups. We observed higher ^{18}F-THK5351 retention in the precentral and postcentral gyri and premotor area in the CBS group than that in the normal control group, while the AD group showed higher ^{18}F-THK5351 retention in the medial and inferior temporal gyri and occipital lobes than the normal control group (uncorrected $p < 0.001$, figure e-2). Compared to the AD group, the CBS group showed higher ^{18}F-THK5351 retention in the bilateral precentral gyrus and right globus pallidus (uncorrected $p < 0.001$, figure e-2) and lower

Table 3 Regional ^{18}F-THK5351 standardized uptake value ratio values in a normal control and patients with corticobasal syndrome

Region	Normal control	CBS	Cohen *d*
R precentral gyrus	1.10 ± 0.08	1.73 ± 0.28	3.86[a]
L precentral gyrus	1.12 ± 0.10	1.81 ± 0.33	3.56[b]
R postcentral gyrus	1.18 ± 0.08	1.50 ± 0.16	2.98[c]
L postcentral gyrus	1.17 ± 0.09	1.54 ± 0.22	2.71[d]
R globus pallidus	3.27 ± 0.42	4.32 ± 0.52	2.46[d]
L globus pallidus	3.25 ± 0.39	4.41 ± 0.66	2.51[d]
R putamen	2.71 ± 0.33	3.42 ± 0.35	2.25
L putamen	2.68 ± 0.32	3.40 ± 0.40	2.24
R caudate nucleus	2.17 ± 0.27	2.22 ± 0.24	0.20
L caudate nucleus	2.14 ± 0.30	2.08 ± 0.34	0.21
R substantia nigra	2.40 ± 0.18	2.81 ± 0.52	1.30
L substantia nigra	2.52 ± 0.20	3.00 ± 0.57	1.37
R middle inferior temporal gyrus	1.56 ± 0.09	1.61 ± 0.10	0.46
L middle inferior temporal gyrus	1.52 ± 0.12	1.62 ± 0.11	0.97
R hippocampus	2.31 ± 0.13	2.36 ± 0.09	0.49
L hippocampus	2.30 ± 0.13	2.31 ± 0.16	0.14
R amygdala	2.50 ± 0.25	2.64 ± 0.40	0.48
L amygdala	2.52 ± 0.24	2.52 ± 0.31	0.00
R superior frontal gyrus	1.29 ± 0.13	1.66 ± 0.14	3.03[b]
L superior frontal gyrus	1.28 ± 0.13	1.69 ± 0.16	3.22[b]
R superior parietal gyrus	1.26 ± 0.11	1.66 ± 0.24	2.63[d]
L superior parietal gyrus	1.25 ± 0.10	1.68 ± 0.16	3.64[b]
R posterior cingulate gyrus	1.54 ± 0.13	1.77 ± 0.12	1.93
L posterior cingulate gyrus	1.52 ± 0.11	1.77 ± 0.09	2.61[d]

Abbreviation: CBS = corticobasal syndrome.
Data are mean ± standard deviation.
[a] $p < 0.0001$.
[b] $p < 0.0005$.
[c] $p < 0.001$.
[d] $p < 0.005$.

^{18}F-THK5351 retention in the parahippocampal gyrus and inferior temporal cortex (data not shown). The β-amyloid burden in the current CBS cases was additionally examined using PiB-PET (table 1). Four out of 5 CBS cases showed no remarkable β-amyloid burden. One CBS case (case 2) showed high β-amyloid burden; however, no remarkable atrophy was observed in the hippocampus of this patient. There were no significant differences in ^{11}C-PiB retention between CBS and normal control groups (tables e-2 and e-3).

DISCUSSION ^{3}H-THK5351 was able to bind to tau deposits in the postmortem brain with CBD (figure 1). Higher accumulation of ^{18}F-THK5351 was seen in the precentral and postcentral gyri, and globus pallidus in patients with CBS than in normal controls (figure 2 and table 3). The spatial patterns of ^{18}F-THK5351 binding were compatible with tau deposit distributions observed in brain autopsies of patients with CBS-CBD,[18] CBS-PSP,[19] and CBS-AD.[20] These results strongly suggest that ^{18}F-THK5351 PET is able to visualize tau deposits in patients with CBS. In the future, image-to-autopsy studies are necessary to validate the binding ability of this tracer to tau lesions in CBD.

We observed that 4 out of 5 CBS cases showed negative amyloid PET scans, indicating that ^{18}F-THK5351 retention in these 4 CBS cases is not likely to reflect concomitant AD pathology. The spatial distribution of ^{18}F-THK5351 uptake differed greatly between CBS and AD cases. No remarkable uptake of ^{18}F-THK5351 was observed in the medial and inferior temporal lobes of patients with CBS (figures 2 and e-2). The findings of CSF analysis also supported that these CBS cases do not have AD pathology. One CBS case (case 2) showed high β-amyloid burden, suggesting that this case is CBS-CBD with incidental or preclinical β-amyloid burden, because β-amyloid burden is observed in 20%–30% of normal elderly individuals.[16,21,22] Another possibility is that this case has AD-related tau deposits in the neocortex, which is comparable to hippocampal sparing AD.[23,24] Our patients with CBS are more likely to be CBS-CBD than CBS-PSP, as their p-tau to total tau ratio in CSF was 0.18 or lower.[25] ^{18}F-THK5351 PET may help to differentiate between CBS-CBD and CBS-PSP. Patients with CBS-CBD show a greater tau burden in the primary motor and somatosensory cortices and in the putamen than those with CBS-PSP.[18] In a future study, the spatial pattern of ^{18}F-THK5351 binding should be compared between CBS-CBD and CBS-PSP cases.

One limitation of this study was that we have not performed postmortem examination in the current CBS cases and could examine only one CBD brain sample from a different patient, owing to the limited availability of well-characterized autopsy samples. Autoradiography with multiple and scanned cases will improve the reliability of ^{18}F-THK5351 PET imaging. Another limitation was the relatively small sample size. We therefore could not examine the association between ^{18}F-THK5351 retention and clinical severity in CBS. Nevertheless, a higher accumulation of ^{18}F-THK5351 was seen in the cortical regions and globus pallidus of the side contralateral to the symptom-predominant side (figure 2, A and B, and table 2), suggesting that the spatial distribution of the tracer signal may explain the clinical symptoms in CBS. ^{18}F-THK5351 retention may not increase in alignment in proportion to the severity of the illness and may change in the same manner as an inverted parabola in response to neuronal cell loss.

^{18}F-THK5351 PET demonstrated high tracer signals in sites susceptible to tau deposition in patients

with CBS. ^{18}F-THK5351 should be considered as a clinical tool in the assessment of tau burden in CBS. Future clinical studies should clarify whether the radiotracer is a suitable biomarker for the early diagnosis and monitoring of disease progression in CBS. ^{18}F-THK5351 may also be a potential tool for monitoring the effects of anti-tau-specific therapeutics in patients with CBS.

AUTHOR CONTRIBUTIONS

Dr. Kikuchi and Dr. Okamura designed the experiments, analyzed and interpreted data, and wrote the manuscript. All authors contributed to the data collection and analysis and reviewed the paper.

ACKNOWLEDGMENT

The authors thank the participants; colleagues involved in this study; Hiroshi Kuroda, Naoki Suzuki, Shuhei Nishiyama, Yoshiki Takai, Rumiko Izumi, Kenta Kawata, Kotaro Komatsu, Ryuhei Harada, Tomoko Totsune, and Kimihiko Kaneko at the Department of Neurology at Tohoku University Hospital; the staff of the Department of Radiology at Tohoku University Hospital; the staff of the Cyclotron and Radioisotope Center at Tohoku University; and Akihisa Saito and Zin-ichi Saito at the Department of Neurology at Saito Hospital for support.

STUDY FUNDING

Supported in part by Grants-in-Aid for Scientific Research (C) (23591266, 26461303) and (B) (24390219) from the Ministry of Education, Culture, Sports, Science and Technology (MEXT) of Japan.

DISCLOSURE

A. Kikuchi received speaker honoraria from Otsuka Pharmaceutical Co., Ltd., Kyowa Hakko Kirin Co., Ltd., and Dainippon Sumitomo Pharma Co., Ltd.; research support from Novartis Pharma K.K. and Takeda Pharmaceutical Co., Ltd.; and Grant-in-Aid for Scientific Research (C) (26461303) from the Ministry of Education, Culture, Sports, Science and Technology (MEXT) of Japan. N. Okamura is a consultant for CLINO Ltd. and has received royalties from GE Healthcare Co., Ltd., speaker honoraria from Eisai Co., Ltd., Nihon Medi-Physics Co., Ltd., Fujifilm RI Pharma Co., Ltd., and Daiichi Sankyo Co., Ltd.; Grant-in-Aid for Scientific Research (B) (15H04900) and for Exploratory Research (16K15570) from the Ministry of Education, Culture, Sports, Science and Technology (MEXT) of Japan; and research grants from SENSHIN Medical Research Foundation, Mitsui Sumitomo Insurance Welfare Foundation, and Japan Research Foundation for Clinical Pharmacology. T. Hasegawa received speaker honoraria from Novartis Pharma K.K., GlaxoSmithKline Pharmaceuticals Co., Ltd., Kyowa Hakko Kirin Co., Ltd., Dainippon Sumitomo Parma Co., Ltd., Otsuka Pharmaceutical Co., Ltd., FP Pharmaceutical Co., Ltd., Eisai Co., Ltd., and Nippon Chemiphar Co., Ltd.; Grant-in-Aid for Scientific Research (C) (26461263) from the Ministry of Education, Culture, Sports, Science and Technology (MEXT) of Japan; and Grant-in-Aid for Practical Research Projects for Rare/Intractable Diseases from Japan Agency for Medical Research and Development (AMED). R. Harada has received travel scholarship from the Human Amyloid Imaging conference and Grants-in-Aid for Scientific Research (15K19767) and JSPS Fellowship from the Ministry of Education, Culture, Sports, Science and Technology (MEXT) of Japan. S. Watanuki has received Grant-in-Aid for Scientific Research (C) (26460717) from the Ministry of Education, Culture, Sports, Science and Technology (MEXT) of Japan. Y. Funaki reports no disclosures relevant to the manuscript. K. Hiraoka has received Grant-in-Aid for Scientific Research (C) (15K08127) from the Ministry of Education, Science and Technology (MEXT) of Japan. T. Baba has received lecture fees from Boehringer Ingelheim Co., Ltd., Novartis Pharma K.K., Eisai Co., Ltd., Daiichi Sankyo Co., Ltd., Kyowa Hakko Kirin Co., Ltd., and Dainippon Sumitomo Pharma Co., Ltd. N. Sugeno received research support from Dainippon Sumitomo Pharma Co., Ltd. R. Oshima, S. Yoshida, J. Kobayashi, M. Ezura, M. Kobayashi, and O. Tano report no disclosures relevant to the manuscript. S. Mugikura has received Grant-in-Aid for Scientific Research from the Ministry of Education, Culture, Sports, Science and Technology (MEXT) of Japan. R. Iwata and A. Ishiki report no disclosures relevant to the manuscript. K. Furukawa received lecturer's fees from Eisai Co., Ltd., Takeda Pharmaceutical Co., Ltd., Novartis Pharma K.K., Daiichi Sankyo Co., Ltd., Ono Pharmaceutical Co., Ltd., and Janssen Pharmaceutical K.K.; served on the editorial boards of *Ageing Research Reviews* and *Geriatrics & Gerontology International*; and received a research grant (15K15268) from the Ministry of Education, Culture, Sports, Science and Technology (MEXT) of Japan. H. Arai reports no disclosures relevant to the manuscript. S. Furumoto is a consultant for CLINO Ltd. and has received research support from CLINO Ltd. and the Industrial Technology Research grant program of the NEDO (09E51025a) of Japan. M. Tashiro received speaker honoraria from GlaxoSmithKline K.K. and Toyota Central R&D Labs., Inc.; serves as a controller and a councilor of the Japanese Society of Nuclear Medicine, a secretary of Japanese Histamine Research Society, and an associate editor of *Annals of Nuclear Medicine*; and has received research support from GlaxoSmithKline K.K., Nihon Medi-Physics Co., Ltd., and the Japan Research Foundation for Clinical Pharmacology, and Grants-in-Aid for Scientific Research from the Ministry of Education, Science and Technology (MEXT) and the Ministry of Health, Labor and Welfare of Japan. K. Yanai has received Scientific Research on Innovative Areas (Brain Protein Aging and Dementia Control) (26117003). Y. Kudo has received research support from GE Healthcare and the SEI (Sumitomo Electric Industries, Ltd.) Group CSR Foundation and the Health and Labor Sciences research grant (12103244) from the Ministry of Health, Labor, and Welfare. A. Takeda served on the scientific advisory board for AbbVie G.K., Ono Pharmaceutical Co., Ltd., Otsuka Pharmaceutical Co., Ltd., Pfizer Pharmaceuticals, and Takeda Pharmaceutical Co., Ltd.; serves as an editorial board member of *Frontiers in Aging Neuroscience*; received honoraria from Daiichi Sankyo Co., Ltd., Dainippon Sumitomo Pharma Co., Ltd., Eisai Co., Ltd., FP Pharmaceutical Corporation, GlaxoSmithKline K.K., Kyowa Hakko Kirin Co., Ltd., Medtronic Japan Co., Ltd., Nippon Boehringer Ingelheim Co., Ltd., and Janssen Pharmaceutical K.K.; and has received Grants-in-Aid for Scientific Research (B) (24390219) from the Ministry of Education, Culture, Sports, Science and Technology (MEXT) of Japan and Scientific Research (15lk0201010h0004) from the Japan Agency for Medical Research and Development (AMED). M. Aoki received funding for travel and speaker honoraria from Eisai Inc., Mitsubishi Tanabe Pharma Corporation, Astellas Pharma Inc., Takeda Pharmaceutical Co. Ltd., Sanofi K.K. Novartis Pharma K.K., and Dainippon Sumitomo Pharma Co. Ltd.; has received research grants for Research on Nervous and Mental Disorders, Research on Rare and Intractable Diseases, and Research on Psychiatric and Neurological Diseases and Mental Health from the Ministry of Health, Labor, and Welfare; and has received Grants-in-Aids for Scientific Research, an Intramural Research Grant for Neurological Psychiatric Disorders from NCNP, and Scientific Research from the Ministry of Education, Culture, Sports, Science and Technology (MEXT) of Japan, and Practical Research Project for Rare/Intractable Diseases from the Japan Agency for Medical Research and Development (AMED). Go to Neurology.org for full disclosures.

Received February 26, 2016. Accepted in final form August 22, 2016.

REFERENCES

1. Rebeiz JJ, Kolodny EH, Richardson EP Jr. Corticodentatonigral degeneration with neuronal achromasia. Arch Neurol 1968;18:20–33.
2. Gibb WR, Luthert PJ, Marsden CD. Corticobasal degeneration. Brain 1989;112:1171–1192.
3. Boeve BF, Lang AE, Litvan I. Corticobasal degeneration and its relationship to progressive supranuclear palsy and frontotemporal dementia. Ann Neurol 2003;54(suppl 5):S15–S19.
4. Lee SE, Rabinovici GD, Mayo MC, et al. Clinicopathological correlations in corticobasal degeneration. Ann Neurol 2011;70:327–340.
5. Shoghi-Jadid K, Small GW, Agdeppa ED, et al. Localization of neurofibrillary tangles and beta-amyloid plaques in

the brains of living patients with Alzheimer disease. Am J Geriatr Psychiatry 2002;10:24–35.
6. Chien DT, Bahri S, Szardenings AK, et al. Early clinical PET imaging results with the novel PHF-tau radioligand [F-18]-T807. J Alzheimers Dis 2013;34:457–468.
7. Maruyama M, Shimada H, Suhara T, et al. Imaging of tau pathology in a tauopathy mouse model and in Alzheimer patients compared to normal controls. Neuron 2013;79:1094–1108.
8. Fodero-Tavoletti MT, Furumoto S, Taylor L, et al. Assessing THK523 selectivity for tau deposits in Alzheimer's disease and non-Alzheimer's disease tauopathies. Alzheimers Res Ther 2014;6:11.
9. Okamura N, Furumoto S, Fodero-Tavoletti MT, et al. Non-invasive assessment of Alzheimer's disease neurofibrillary pathology using 18F-THK5105 PET. Brain 2014;137:1762–1771.
10. Harada R, Okamura N, Furumoto S, et al. [18F]THK-5117 PET for assessing neurofibrillary pathology in Alzheimer's disease. Eur J Nucl Med Mol Imaging 2015;42:1052–1061.
11. Harada R, Okamura N, Furumoto S, et al. 18F-THK5351: a novel PET radiotracer for imaging neurofibrillary pathology in Alzheimer's disease. J Nucl Med 2016;57:208–214.
12. Kepe V, Bordelon Y, Boxer A, et al. PET imaging of neuropathology in tauopathies: progressive supranuclear palsy. J Alzheimers Dis 2013;36:145–153.
13. Okamura N, Furumoto S, Harada R, et al. Novel 18F-labeled arylquinoline derivatives for noninvasive imaging of tau pathology in Alzheimer disease. J Nucl Med 2013;54:1420–1427.
14. Mathew R, Bak TH, Hodges JR. Diagnostic criteria for corticobasal syndrome: a comparative study. J Neurol Neurosurg Psychiatry 2012;83:405–410.
15. Bourgeat P, Chetelat G, Villemagne VL, et al. Beta-amyloid burden in the temporal neocortex is related to hippocampal atrophy in elderly subjects without dementia. Neurology 2010;74:121–127.
16. Villemagne VL, Pike KE, Chetelat G, et al. Longitudinal assessment of Abeta and cognition in aging and Alzheimer disease. Ann Neurol 2011;69:181–192.
17. Schoonenboom NS, Reesink FE, Verwey NA, et al. Cerebrospinal fluid markers for differential dementia diagnosis in a large memory clinic cohort. Neurology 2012;78:47–54.
18. Kouri N, Murray ME, Hassan A, et al. Neuropathological features of corticobasal degeneration presenting as corticobasal syndrome or Richardson syndrome. Brain 2011;134:3264–3275.
19. Tsuboi Y, Josephs KA, Boeve BF, et al. Increased tau burden in the cortices of progressive supranuclear palsy presenting with corticobasal syndrome. Mov Disord 2005;20:982–988.
20. Okazaki K, Fu YJ, Nishihira Y, et al. Alzheimer's disease: report of two autopsy cases with a clinical diagnosis of corticobasal degeneration. Neuropathology 2010;30:140–148.
21. Rowe CC, Ng S, Ackermann U, et al. Imaging beta-amyloid burden in aging and dementia. Neurology 2007;68:1718–1725.
22. Aizenstein HJ, Nebes RD, Saxton JA, et al. Frequent amyloid deposition without significant cognitive impairment among the elderly. Arch Neurol 2008;65:1509–1517.
23. Murray ME, Graff-Radford NR, Ross OA, Petersen RC, Duara R, Dickson DW. Neuropathologically defined subtypes of Alzheimer's disease with distinct clinical characteristics: a retrospective study. Lancet Neurol 2011;10:785–796.
24. Malkani RG, Dickson DW, Simuni T. Hippocampal-sparing Alzheimer's disease presenting as corticobasal syndrome. Parkinsonism Relat Disord 2012;18:683–685.
25. Aerts MB, Esselink RA, Bloem BR, Verbeek MM. Cerebrospinal fluid tau and phosphorylated tau protein are elevated in corticobasal syndrome. Mov Disord 2011;26:169–173.